First-Principles Determination of Chain-Structure Instability in $KNbO_3$

Rici Yu and Henry Krakauer
Department of Physics, College of William and Mary, Williamsburg, Virginia 23187-8795
(Received 21 December 1994)

A complete mapping in the Brillouin zone of the structural instability associated with the ferroelectric phase transitions of $KNbO_3$ has been obtained by first-principles calculations using a linear response approach. The wave-vector dependence of the instability reveals pronounced two-dimensional character, which corresponds to chains oriented along ⟨100⟩ directions of displaced Nb atoms. The results are discussed in relation to models of the ferroelectric phase transitions.

PACS numbers: 77.80.–e, 63.20.–e, 64.60.–i

Potassium niobate ($KNbO_3$) is one of the most extensively studied systems of the perovskite family of ferroelectric materials. Like $BaTiO_3$, it crystallizes in the simple cubic perovskite structure at high temperatures (above 710 K for $KNbO_3$), and undergoes three ferroelectric phase transitions at lower temperatures, resulting in a series of distorted perovskite structures: the tetragonal phase, the orthorhombic phase, and the ground-state rhombohedral phase [1]. The character of the phase transitions in these two systems is therefore expected to be similar. Attempts to understand the origin of these phase transitions were initially shaped by "soft-phonon" models [1]. This theory considers the transitions as displacive and induced by the softening of a zone-center TO mode as the transition temperature is approached. These models were successful in explaining measured temperature dependent changes of the soft-phonon frequency and polarizability as the transition temperature is approached from above [1]. Somewhat later, however, Comes, Lambert, and Guinier [2] suggested that the transitions may be of the order-disorder type, introducing the eight-site model to explain diffuse x-ray scattering patterns in the orthorhombic phase of $KNbO_3$. The interpretation of the streak pattern in terms of disorder has been disputed by Hüller [3], who attributed it instead to dynamical scattering. A more recent experimental investigation of the diffuse x-ray scattering by Holma, Takesue, and Chen [4] concluded that the results were in better agreement with the dynamical interpretation. However, there have been other experiments [5] that provided support for the role of disorder in the high-temperature phases. Thus, although these perovskite systems have been studied for decades, the structure of the high-temperature phases and the related character of the phase transitions continue to be a source of controversy, with contradictory evidence for quasistatic disorder versus soft-mode behavior.

In this Letter, we report first-principles lattice dynamics calculations for the ideal cubic perovskite structure of $KNbO_3$, using a linear response approach within the framework of the linearized augmented plane-wave (LAPW) method [6]. The linear response approach greatly reduces the computational burden in mapping out phonon dispersions in the full Brillouin zone (BZ). Most theoretical work has been concerned with the zone-center phonon instability, which is associated with the phase transitions, much of it based on empirical or model calculations. To understand the possible roles of disorder and dynamical scattering, however, one needs to know the energetics of the these systems throughout the BZ. This problem has only been addressed by model calculations (e.g., see Ref. [7]). First-principles local-density-approximation (LDA) calculations have recently been applied to study the basic electronic, structural, and dynamical properties of the perovskites [8–10], but the computational inefficiency of the traditional supercell approach makes it difficult to calculate phonon frequencies at other than a few high-symmetry points. The results of our calculations show a soft-phonon dispersion that exhibits an instability of a pronounced two-dimensional nature and suggests a one-dimensional chain-type instability.

The calculations were performed at the experimental lattice constant (extrapolated to zero temperature), $a = 4.016$ Å. A special k-point $4 \times 4 \times 4$ grid [11] was used for k-point summation in the self-consistent calculations. (We have calculated the phonon frequencies at the zone center with the $6 \times 6 \times 6$ grid. The soft-mode frequency was found to become more unstable by about $50i$ cm^{-1} while the other modes are relatively unaffected.) The Wigner interpolation formula [12] was used for the exchange-correlation potential. Pseudopotentials were used to exclude the tightly bound core states, which improves the numerical stability of the calculated forces [6]. The relatively loosely bound K($3s$) and Nb($4s$, $4p$) states were pseudized and included in the lower window of a two-window calculation. Approximately 540 LAPW basis functions are used at each k point. Phonon dispersions in the harmonic approximation were obtained in the full BZ as follows. First, *ab initio* calculations were carried out to determine the dynamical matrix at ten irreducible phonon wave vectors of a $4 \times 4 \times 4$ uniform mesh, which by symmetry gives the dynamical matrix at all mesh points. Interpolation is then performed which properly takes into account the LO-TO splitting at the zone center by separating the dynamical matrix into

0031-9007/95/74(20)/4067(4)$06.00

a long-range dipole-dipole term and a short-range term [13]. The former is obtained from the calculated Born effective charges and dielectric constant using the Ewald summation technique. The remaining short-range part is then interpolated using real-space force constants, which are found through Fourier transform for atoms within two unit cells of each other in each direction. The linear response approach also makes possible the calculation of the dielectric constant and the Born effective charges, which are necessary for this procedure.

We first present results that can be compared with previous calculations and experiment. Table I compares our dielectric constant to experiment and our calculated Born effective charges to those obtained previously by the Berry's phase calculations of Resta, Posternak, and Baldereschi [14] using the LAPW method and by Zhong, King-Smith, and Vanderbilt [15] using a plane-wave pseudopotential method. Our calculated dielectric constant, $\varepsilon_\infty = 6.34$, overestimates the experimental value, $\varepsilon_\infty = 4.69$, a well-known tendency of the LDA even in simpler materials [16]. The high symmetry of the cubic perovskite structure results in an isotropic effective charge tensor for the K and Nb atoms, but the lower site symmetry of the oxygens results in two distinct diagonal values—for displacements along and perpendicular to the Nb-O bonds, labeled 1 and 2, respectively. There is generally good agreement between these different calculations for the effective charges. In particular, they all yield large values for Z^*(Nb) and Z_1^*(O). The origin of these large values is the large covalent interactions between the transition-metal and oxygen atoms in these materials [8]. This has been convincingly demonstrated recently by Posternak, Resta, and Baldereschi [17]. Table II compares phonon frequencies at the Γ point with the frozen-phonon LAPW calculations of Singh and Boyer [9] and Zhong, King-Smith, and Vanderbilt [15]. All the calculations find unstable TO modes at the Γ point with similar imaginary frequencies corresponding to the observed soft mode. The LO mode frequencies were obtained from the following dynamical matrix:

$$D^{\mathrm{LO}}_{i\alpha,j\beta} = D^{\mathrm{TO}}_{i\alpha,j\beta} + \frac{4\pi e^2}{\sqrt{M_i M_j}\,\Omega}\,\frac{(\mathbf{Z}_i^*\cdot\hat{\mathbf{q}})_\alpha (\mathbf{Z}_j^*\cdot\hat{\mathbf{q}})_\beta}{\varepsilon_\infty}, \quad (1)$$

TABLE I. Comparison of calculated Born effective charges in $KNbO_3$.

	LAPW-LR	LAPW[a]	PW[b]
Z^*(K)	1.14	0.82	1.14
Z^*(Nb)	9.37	9.13	9.23
Z_1^*(O)	−6.86	−6.58	−7.01
Z_2^*(O)	−1.65	−1.68	−1.68
ε_∞	6.34		4.69[c]

[a]Reference [14].
[b]Reference [15].
[c]Derived from experiment.

TABLE II. Comparison of our calculated Γ-point phonon frequencies (cm^{-1}) in $KNbO_3$ with LAPW and plane-wave frozen-phonon calculations and experiment.

LAPW-LR	LAPW[a]	PW[b]	Experiment[c]
TO modes			
147*i*	115*i*	143*i*	Soft
170	168	188	198
477	483	506	521
262	266		280[d]
LO modes			
168		183	190
405		407	418
743		899	826

[a]Reference [10].
[b]Reference [15].
[c]Reference [18].
[d]Measured in the tetragonal phase, $T = 585$ K.

where D^{TO} is the zone-center dynamical matrix without macroscopic field, $\mathbf{Z}_i^*$ (M_i) is the Born effective charge tensor (mass) of atom i, Ω is the unit cell volume, α, β are Cartesian indices, and $\hat{\mathbf{q}}$ is a unit wave vector. All LO modes were found to be stable due to the contribution of the macroscopic field. (The last TO mode is infrared inactive, and thus does not exhibit LO-TO splitting.) The results of Zhong, King-Smith, and Vanderbilt employed $\varepsilon_\infty = 4.69$, extracted from experiment, whereas we used our larger calculated dielectric constant.

The calculated phonon dispersion curves are plotted along high-symmetry directions in Fig. 1, using the real space force constants as discussed above. The ΓX, ΓM, and ΓR lines are along the ⟨100⟩, ⟨110⟩, and ⟨111⟩ directions, respectively. Imaginary phonon frequencies (of unstable modes) are represented as negative values. We will be mainly concerned with the "soft" modes, as these are relevant to the phase transitions. As seen in Fig. 1, there are two modes that are unstable along the ΓX direction. These are TO modes that involve

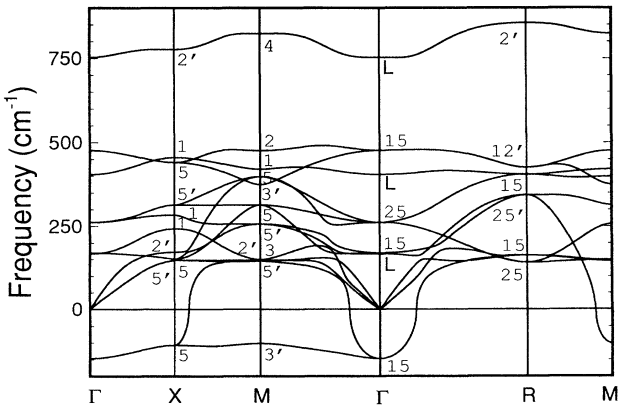

FIG. 1. Calculated phonon dispersions of $KNbO_3$ in the ideal cubic structure at the experimental lattice constant. The letter L indicates longitudinal modes at the zone center.

largely the motion of the Nb and O atoms along the ⟨100⟩ directions. One of these modes remains unstable along ΓM and MX directions. Examination of the eigenvectors reveals that it is polarized along ⟨100⟩. The other TO mode, which now cannot remain polarized along ⟨100⟩, stabilizes rapidly away from the ΓX direction. Along ΓR and MR, the unstable mode(s) again stiffen up rapidly away from Γ and M points, as the polarizations deviate from the ⟨100⟩ directions. Thus an unstable mode arises for all wave vectors perpendicular to the ⟨100⟩ directions, i.e., in the {100} planes, with the displacements parallel to these directions. Away from these planes, the frequency of this mode rises rapidly and becomes stable at about one-fifth of the way to the zone boundary. This pronounced two-dimensional instability is better visualized in Fig. 2, in which the frequency isosurface of the lowest unstable phonon branch corresponding to $\omega = 0$ is shown. (The cubic BZ is outlined by the straight lines.) The region of instability, $\omega^2(\mathbf{q}) < 0$, lies between the three pairs of nearly flat planes, which are parallel to the surfaces of the cube. (Isosurfaces for negative values of ω^2 look qualitatively similar but with opposite planes closer to each other.) The phonon dispersions as given in Fig. 1 cannot be directly compared with experiment, in part because there are little data for the cubic phase. In addition, all experimentally observed vibrational excitations have positive frequency, of course, as a result of either anharmonic stabilization or because of static or quasistatic disorder. These issues are discussed further below.

The instability can be traced primarily to particular elements of the dynamical matrix involving Nb atom displacements along the ⟨100⟩ directions. Figure 3 depicts a diagonal element of the dynamical matrix, $D_{zz}(\mathrm{Nb})$, in the form of isosurfaces in the BZ. The k_z direction is oriented vertically in this figure. The first pair of surfaces (with sheets near the top and bottom of the figure and displaying a sharp cusp) are for a positive (stable) value of this matrix element. (The cusps result from the dipole-dipole interaction which makes the dynamical matrix nonanalytic near the zone center.) The other, flatter sheets are $D_{zz}(\mathrm{Nb}) = 0$ isosurfaces that sandwich a region where the matrix element is negative, i.e., where the z displacement of Nb atoms is unstable. The near two dimensionality of the instability is thus also revealed in these isosurfaces. Since the Nb atom displacements are along the z direction, this figure clearly shows that only nearly transverse displacements are unstable.

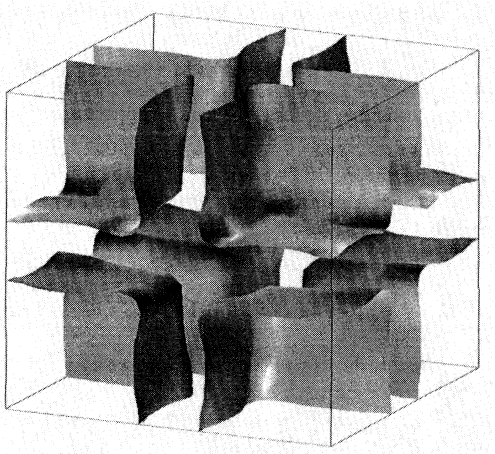

FIG. 2. Zero-frequency isosurface of the lowest unstable phonon branch over the BZ. The mode is unstable in the region between the nearly flat surfaces. Γ is located at the center of the cube.

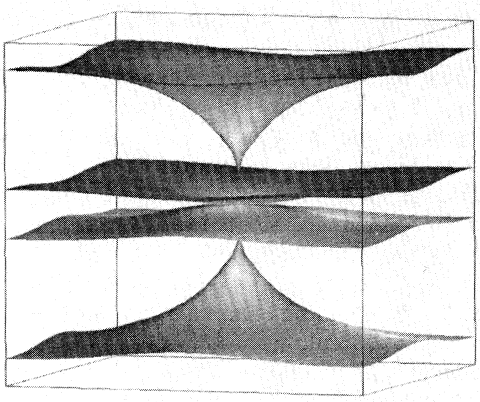

FIG. 3. Isosurfaces of the dynamical matrix element $D_{zz}(\mathrm{Nb})$ over the BZ. The central pair of surfaces, $D_{zz}(\mathrm{Nb}) = 0$, separates the unstable (between the two surfaces) and stable regions. The other pair of surfaces is for a positive value (1.1×10^5 cm^{-2}).

We now consider the implication of the above results for the unstable modes, which can be summarized briefly as follows: (1) there exist unstable modes in and near the $k_z = 0$ (and equivalent) planes with the polarizations perpendicular to the planes, (2) the modes show little dispersion in the planes, whereas they stabilize rapidly away from the planes (nearly two-dimensional behavior), and (3) the instability is largely inherent in the subsystem of Nb atoms in the background of fixed K and O atoms. Since the unstable modes are not very dispersive in the ⟨100⟩ planes, any linear combination of these modes will also be comparably unstable. A linear combination within one of the planar slablike regions in Fig. 2 can thus yield a *localized* chain that is unstable. For example, a planar average over the $k_z = 0$ plane would yield a single infinite chain oriented along the [001] direction of Nb atoms coherently displaced by the same amount along the chain direction. Although chains of infinite length are the most unstable, finite-length chains can also be unstable. From the thickness of the slab region that contains the instability (Fig. 2), we estimate the length of the shortest chains to be approximately $5a \simeq 20$ Å. Such chains are then the basic unit of instability; a smaller unit, such as a

single Nb atom, would not be unstable, as least for small displacements.

The linear response results presented here include only the harmonic terms of the Born-Oppenheimer potential expanded about the ideal cubic structure. The character of the ferroelectric phase transition depends crucially on the anharmonic terms, however. Specifically, the depth of the Born-Oppenheimer potential wells associated with the chain instability discussed above is determined by anharmonicity. In principle, the well depths associated with the chain instability could be computed in a supercell calculation, but this is difficult because it requires using large supercells containing many formula units. In any case, such potential wells are likely to be of the same order of magnitude as that for the zone-center displacements. Unfortunately, calculations for the zone-center modes [8,9] found the well depths to be very sensitive to the volume at which the calculation was performed, with changes as small as a 1% contraction of the lattice parameter eliminating the well depth completely. Since the accuracy of the LDA for lattice parameters is approximately in this range, there is considerable uncertainty regarding the magnitude of the well depths. We can, however, consider the implications of our results in two limiting cases for the unknown well depths. If the well depths are shallow, on the scale $k_B T_c$ and/or the zero-point energy of the Nb atoms, then it is likely that the unstable modes in Fig. 1 are anharmonically stabilized, with atoms vibrating at renormalized positive frequencies. This is the conventional soft-mode picture. Experimental observations of the soft mode and its temperature dependence are in qualitative agreement with the anisotropic dispersion in our calculation. The best available experimental results on the temperature dependence of phonon dispersion in the cubic phase appear to be for $KTaO_3$ [19,20], which is an incipient ferroelectric and is devoid of the strong damping that is present in $KNbO_3$ and $BaTiO_3$. Figure 2 of Ref. [20] clearly shows that temperature dependence of the TO mode is large only for wave vectors near the zone center along [111]. This is not the case along [100] and [110]: Although the observed soft TO mode does not show much temperature dependence near the zone boundary, there is significant temperature dependence in other modes, particularly, the observed TA mode. This behavior can possibly be interpreted as resulting from the mixing of the TO and TA modes as a result of anharmonic renormalization.

The order-disorder model cannot be excluded by the results of the present work, however. If the potential wells are deep, the Nb atoms would have a strong tendency to stay close to the bottoms of the potential wells rather than oscillating about its ideal position, even in the high-temperature phases. The ferroelectric phase transitions would then be of the order-disorder type. In this case, the chain-structure instability deduced from our calculated phonon dispersion can be seen to be consistent with the eight-site model proposed by Comes, Lambert, and Guinier [2]. For instance, their orthorhombic structure corresponds to chains oriented along [001] displaced either in the $+z$ or $-z$ direction, but with superimposed chains oriented along [100] ([010]) all having the same displacement in the $+x$ ($+y$) direction, resulting in an average polarization along the [110] direction.

In summary, a first-principles calculation of the lattice dynamics of $KNbO_3$ reveals structural instabilities with pronounced two-dimensional character in the Brillouin zone, corresponding to chains of displaced Nb atoms oriented along the $\langle 100 \rangle$ directions. It seems likely that the dynamics of the phase transitions will involve fluctuations of such chains, although the full implications of this unusual instability on the structure of the high-temperature phases and the character of the ferroelectric phase transitions remain to be explored.

Supported by Office of Naval Research Grant No. N00014-94-1-1044. Computations were carried out at the Cornell Theory Center. We are pleased to acknowledge helpful interactions with Cheng-Zhang Wang.

[1] M. E. Lines and A. M. Glass, *Principles and Applications of Ferroelectrics and Related Materials* (Clarendon Press, Oxford, 1977), and references therein.
[2] R. Comes, M. Lambert, and A. Guinier, Solid State Commun. **6**, 715 (1968).
[3] A. Hüller, Solid State Commun. **7**, 589 (1969).
[4] M. Holma, N. Takesue, and H. Chen, Ferroelectrics (to be published).
[5] T. P. Dougherty, G. P. Wiederrecht, K. A. Nelson, M. H. Garrett, H. P. Jensen, and C. Warde, Science **258**, 770 (1992), and references therein.
[6] R. Yu and H. Krakauer, Phys. Rev. B **49**, 4467 (1994).
[7] A. Hüller, Z. Phys. **220**, 145 (1969).
[8] R. E. Cohen and H. Krakauer, Phys. Rev. B **42**, 6416 (1990); R. E. Cohen, Nature (London) **358**, 136 (1992).
[9] D. J. Singh and L. L. Boyer, Ferroelectrics **136**, 95 (1992).
[10] R. D. King-Smith and D. Vanderbilt, Phys. Rev. B **49**, 5828 (1994).
[11] H. J. Monkhorst and J. D. Pack, Phys. Rev. B **13**, 5188 (1976).
[12] E. Wigner, Phys. Rev. **46**, 1002 (1934).
[13] P. Giannozzi, S. De Gironcoli, P. Pavone, and S. Baroni, Phys. Rev. B **43**, 7231 (1991).
[14] R. Resta, M. Posternak, and A. Baldereschi, Phys. Rev. Lett. **70**, 1010 (1993).
[15] W. Zhong, R. D. King-Smith, and D. Vanderbilt, Phys. Rev. Lett. **72**, 3618 (1994).
[16] A. Dal Corso, S. Baroni, and R. Resta, Phys. Rev. B **49**, 5323 (1994).
[17] M. Posternak, R. Resta, and A. Baldereschi, Phys. Rev. B **50**, 8911 (1994).
[18] M. D. Fontana, G. Metrat, J. L. Servoin, and F. Gervais, J. Phys. C **16**, 483 (1984).
[19] J. D. Axe, J. Harada, and G. Shirane, Phys. Rev. B **1**, 1227 (1970).
[20] C. H. Perry, R. Currat, H. Buhay, R. M. Migoni, W. G. Stirling, and J. D. Axe, Phys. Rev. B **39**, 8666 (1989).

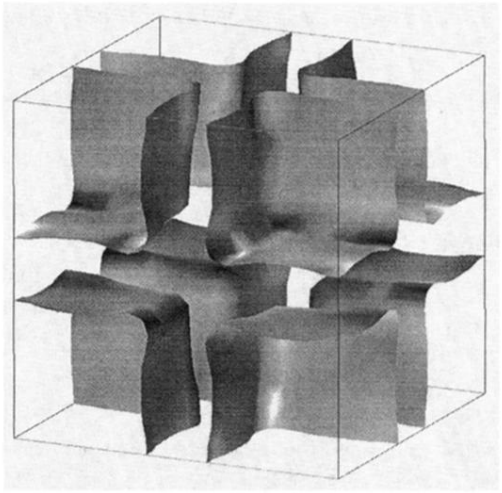

FIG. 2. Zero-frequency isosurface of the lowest unstable phonon branch over the BZ. The mode is unstable in the region between the nearly flat surfaces. Γ is located at the center of the cube.

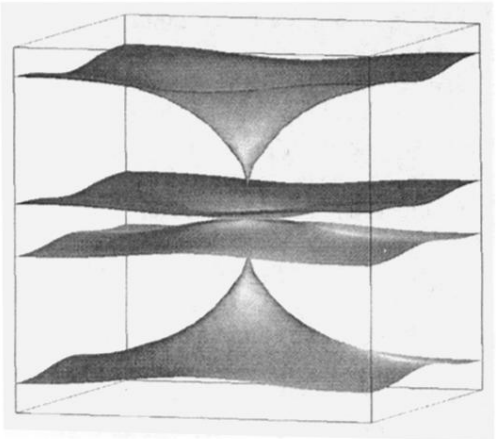

FIG. 3. Isosurfaces of the dynamical matrix element $D_{zz}(\mathrm{Nb})$ over the BZ. The central pair of surfaces, $D_{zz}(\mathrm{Nb}) = 0$, separates the unstable (between the two surfaces) and stable regions. The other pair of surfaces is for a positive value (1.1×10^5 cm^{-2}).